Electronic and Vibrational Spectroscopy of *cis*-Diisothiocyanato(1,4,8,11-tetraazacyclotetradecane)chromium(III) Thiocyanate

Jong-Ha Choi* and Yu Chul Park†

Department of Chemistry, Andong National University, Andong 760-749, Korea
†Department of Chemistry, Kyungpook National University, Daegu 702-701, Korea
Received August 7, 2002

The emission and excitation spectra of *cis*-[Cr(cyclam)(NCS)$_2$]NCS (cyclam = 1,4,8,11-tetraazacyclotetradecane) taken at 77 K are reported. The infrared and visible spectra at room temperature are also measured. The vibrational intervals due to the electronic ground state are extracted from the far-infrared and emission spectra. The ten pure electronic origins due to spin-allowed and spin-forbidden transitions are assigned by analyzing the absorption and excitation spectra. Using the observed transitions, a ligand field analysis has been performed to determine the bonding properties of the coordinated ligands in the title chromium(III) complex. According to the results, it is found that nitrogen atoms of the cyclam ligand have a strong σ-donor character, while the NCS ligand has medium σ- and π-donor properties toward chromium(III) ion.

Key Words : Electronic transitions, Vibrational intervals, Chromium(III) complex, Ligand field analysis

Introduction

In the past several years, the preparation,[1,2] kinetics,[3] photochemistry,[4,5] photophysics[6,7] and structural analysis[8-10] of the *cis*-diacidochromium(III) complexes containing the tetradentate macrocyclic ligand cyclam (1,4,8,11-tetraazacyclotetradecane) have been studied extensively. We also have described the vibrational and electronic energy levels based on the emission, far-infrared and electronic spectroscopy.[11-18] The application of electronic spectroscopy to chromium(III) complexes promises to provide information concerning metal-ligand bonding properties as well as molecular geometry.[1,2] With the use of excitation or absorption spectroscopy the narrow intraconfigurational transitions due to the spin-forbidden in chromium(III) system can be located with a precision two orders of magnitude greater than can the broad spin-allowed bands. Especially, the splittings of sharp-line electronic transitions are very sensitive to the exact bond angles around the metal. Thus it is possible to extract structural information from the electronic spectroscopy without a full X-ray structure determination.[19,20]

The NCS group may coordinate to a transition metal through the nitrogen or the sulfur or both. In general, Cr, Ni and Co metals tend to form M-N bonds, where as metals of the second transition series, such as Rh, Pd and Ir tend to form M-S bonds.[21] However, the oxidation state of the metal, the nature of other ligands in a complex and steric factor also influence the mode of coordination. When the isothiocyanato group coordinates to a chromium(III) ion, it is found that the Cr-N-C and N-C-S angles fall in the range 172.5°-173.5° and 177.2°-179.6°, respectively.[10] So far literature give no information on the detailed ligand field properties of coordinated atoms in the title chromium(III) complex.

*Corresponding author. Phone: +82-54-820-5458; Fax: +82-54-823-1627; E-mail: jhchoi@andong.ac.kr

In this work the 77 K emission and excitation spectra, and the room temperature infrared and visible spectra of *cis*-[Cr(cyclam)(NCS)$_2$](NCS) have been measured. The vibrational intervals of the electronic ground state were determined from the far-infrared and emission spectra. The pure electronic origins were assigned by analyzing the absorption and excitation spectra. With the electronic transitions, a ligand field analysis was performed to determine the metal-ligand bonding properties for the coordinated atoms of isothiocyanato and cyclam ligands toward chromium(III) ion.

Experimental Section

The free ligand cyclam was purchased from Strem Chemicals. All chemicals were reagent grade materials and used without further purification. The *cis*-[Cr(cyclam)(NCS)$_2$](NCS) was prepared as described in the literature.[1]

The far-infrared spectrum in the region 600-50 cm^{-1} was recorded with a Bruker 113v spectrometer on a microcrystalline sample pressed into a polyethylene pellet. The mid-infrared spectrum was obtained with a Mattson Infinities series FT-IR spectrometer using a KBr pellet. The room-temperature visible absorption spectrum was recorded with a HP 8453 diode array spectrophotometer. The emission and excitation spectra at 77 K were measured on a Spex Fluorolog-2 spectrofluorometer. The Nitrogen Dewar accessory was used for the low-temperature scan.[21,22]

Results and Discussion

Absorption Spectrum. The visible absorption spectrum (solid line) of *cis*-[Cr(cyclam)(NCS)$_2$]$^+$ in aqueous solution at room temperature is represented in Figure 1.

It exhibits two bands, one at 20410 cm^{-1} (ν_1) and the other at 27025 cm^{-1} (ν_2), corresponding to the $^4A_{2g} \rightarrow {}^4T_{2g}$ and

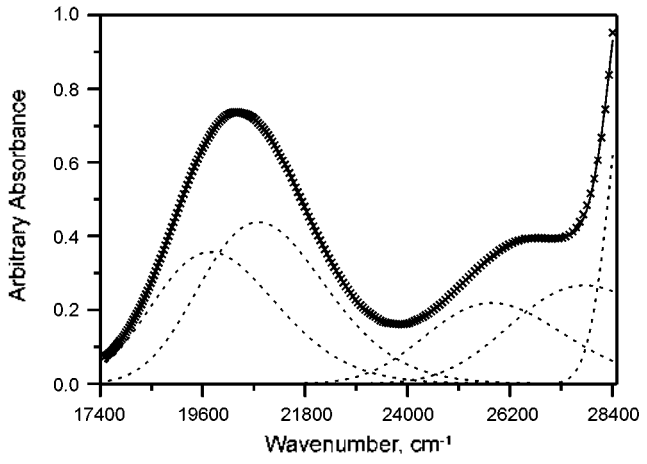

Figure 1. Resolved electronic absorption spectrum of *cis*-[Cr(cyclam)(NCS)$_2$]$^+$ in aqueous solution at 298 K.

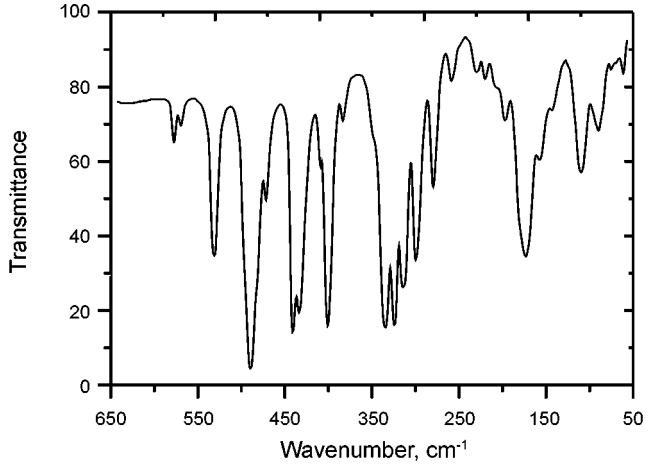

Figure 2. Far-infrared spectrum of *cis*-[Cr(cyclam)(NCS)$_2$](NCS) at 298 K.

$^4A_{2g} \rightarrow {}^4T_{1g}$ (O_h) transitions, respectively.[23-25] The quartet bands have nearly symmetric profiles. In order to have some point of reference for the splittings of the two bands, we have fit the band profiles to four Gaussian curves, as seen in Figure 1. The contribution from outside bands was corrected for fine deconvolution. A deconvolution procedure[26] on the experimental band pattern yielded maxima at 19765, 20795, 25840 and 27810 cm^{-1} for the noncubic split levels of $^4T_{2g}$ and $^4T_{1g}$, respectively. These resolved peak positions were used as the observed spin-allowed transition energies in the ligand field optimization. In fact, using just one Gaussian curve instead of two yields a least squares error only four times that of the best fit (dotted line) shown in Figure 1.

Infrared Spectra. The infrared spectroscopy is useful in assigning configuration of *cis* and *trans* isomers of cyclam chromium(III) complexes. It is well known that *cis* isomer exhibits at least three bands in the 890-830 cm^{-1} region due to the N-H wagging modes while the methylene vibration split into two peaks in the 830-790 cm^{-1} region.[1] However, *trans* isomer shows two groups of bands, a doublet near 890 cm^{-1} arising from the secondary amine vibration and only one band near 810 cm^{-1} due mainly to the methylene vibration.[2,21] The present complex exhibits three bands at 892, 861 and 850 in the N-H wagging frequency region. Two CH_2 rocking bands at 797 and 808 cm^{-1} are also observed. These vibrational modes are not affected by differing counteranions. The infrared spectrum of the title complex was clearly consistent with the *cis* configuration.

Metal-ligand stretching bands occur in the far infrared range. The far-infrared spectrum of *cis*-[Cr(cyclam)(NCS)$_2$](NCS) recorded at room temperature are presented in Figure 2.

The peaks in the range 471-408 cm^{-1} can be assigned to the Cr-N (cyclam) stretching mode.[11,21] A number of absorption bands below 399 cm^{-1} arise from lattice vibration, skeletal bending and the Cr-NCS stretching modes.

Emission Spectrum. An experimental problem lies with the difficulty in distinguishing pure electronic components from the vibronic bands that also appear in the excitation spectrum. It is required that the vibrational intervals of the

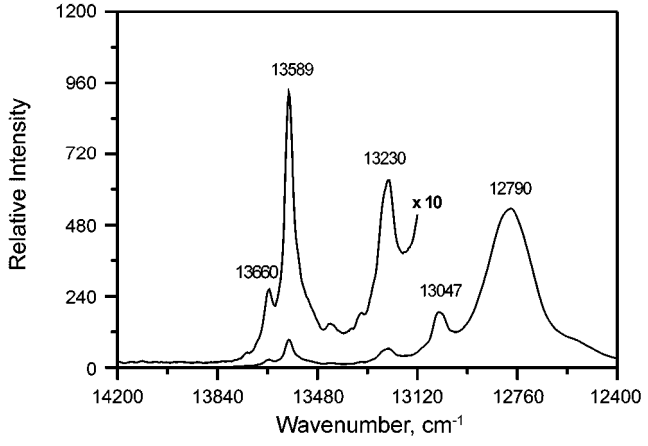

Figure 3. The 19920 cm^{-1} excited emission spectrum of *cis*-[Cr(cyclam)(NCS)$_2$](NCS) at 77 K.

electronic ground state be obtained by comparing the emission spectrum with far-infrared spectral data. The 19920 cm^{-1} (502 nm) excited 77 K emission spectrum of *cis*-[Cr(cyclam)(NCS)$_2$](NCS) is shown in Figure 3. The band positions relative to the lowest zero phonon line, R_1, with corresponding infrared frequencies, are listed in Table 1. The emission spectrum was independent of the exciting wavelength within the first spin-allowed transition region.

The strongest peak at 13589 cm^{-1} is assigned as the zero-phonon line, R_1, because a corresponding strong peak is found at 13602 cm^{-1} in the excitation spectrum. A hot band at 13660 cm^{-1} may be assigned to the second component of the $^2E_g \rightarrow {}^4A_{2g}$ transition. The vibronic intervals occurring in the spectrum consist of several modes that can be presumed to involve primarily ring torsion and angle-bending modes with frequencies in the range 150-264 cm^{-1}. The band at 424 cm^{-1} can be assigned to a Cr-N(cyclam) stretching mode.

Excitation Spectrum. The 77 K excitation spectrum is shown in Figure 4. It was recorded by monitoring a relatively strong vibronic peak in the emission spectrum. The spectrum obtained was independent of the vibronic peak used to monitor it. The peak positions and their assignments are

Table 1. Vibrational frequencies from the 77 K Emission and 298 K infrared spectra for *cis*-[Cr(cyclam)(NCS)$_2$](NCS)[a]

Emission[b]	Infrared	Assignment
-71 w		R_1
0 vs		R_2
	60 w, 74 m, 109 s	Lattice vib., skeletal bends and ν(Cr-NCS)
150 w	156 vw, 174 s, 195 w	
214 vw	205 vw, 221 w, 231 w	
264 w	259 m, 280 s, 300 s	
359 m	312 m, 322 s, 331 s, 346 w	
	386 w, 399 vs	
424 vw	408 sh, 431 m, 439 sh	ν(Cr-N) and ν(NCS)
	471 m, 488 vs	
542 vs	531 vs, 572 w, 580 m	ν(Cr-N)+ring def.
	616 w, 662 w, 695 w	
799 vs	757 m, 797 m, 808 w	δ(CH$_2$)
	850 m, 861 m, 892 m	γ(NH)
	923 m, 1004 vs	
1016 sh	1030 vs, 1056 vs	

[a]Data in cm^{-1}. [b]Measured from zero-phonon line at 13589 cm^{-1}.

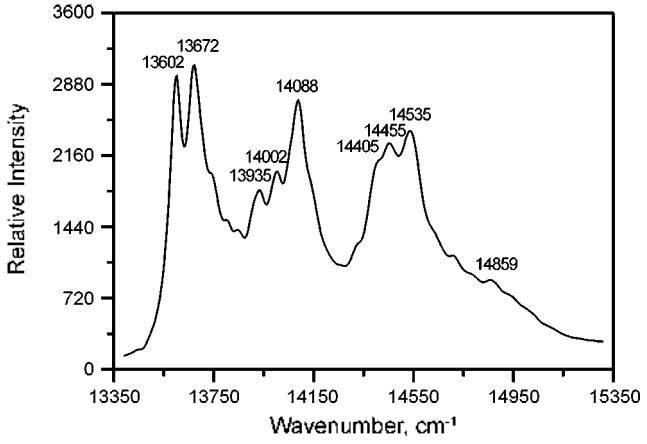

Figure 4. The 12804 cm^{-1} monitored excitation spectrum of *cis*-[Cr(cyclam)(NCS)$_2$](NCS) at 77 K.

tabulated in Table 2. The calculated frequencies in parentheses were obtained by using the vibrational modes ν_1-ν_5 listed in Table 2.

Two strong peaks at 13602 and 13672 cm^{-1} in the excitation spectrum are assigned to the two components (R_1 and R_2) of the $^4A_{2g} \rightarrow {}^2E_g$ transition. The lowest-energy zero-phonon line coincides with the emission origin within 3 cm^{-1}. The zero-phonon line in the excitation spectrum splits into two components 70 cm^{-1} apart, and it can be compared with those[11-18] of the *cis*-[Cr(cyclam)X$_2$]$^{n+}$ system (X = NH$_3$, en/2, pn/2, F$^-$, Cl$^-$, Br$^-$, N$_3^-$, ONO$^-$, ONO$_2^-$), as shown in Table 3. In general, it is not easy to locate positions of the other electronic components because the vibronic sidebands of the ^2E_g levels overlap with the zero phonon lines of $^2T_{1g}$. However, the three components of the $^4A_{2g} \rightarrow {}^2T_{1g}$ electronic origin (T_1, T_2 and T_3) can be found with strong intensities 803, 853 and 933 cm^{-1} from the lowest electronic line, R_1 because the vibronic satellites based on these origins also

Table 2. Peak positions in the 77 K sharp-line excitation spectrum of *cis*-[Cr(cyclam)(NCS)$_2$](NCS)[a]

-13602	Assignment	Calcd[b]		Vibronic frequencies	Ground state frequencies[c]
0 vs	R_1		ν_1	173	173
70 vs	R_2		ν_2	259	251
199 sh			ν_3	325	328
245 ws	$R_2 + \nu_1$	(243)	ν_4	489	485
333 m	$R_1 + \nu_3$	(328)	ν_5	542	549
400 m	$R_2 + \nu_3$	(398)			
486 vs	$R_1 + \nu_4$	(485)			
534 sh	$R_1 + \nu_5$	(549)			
550 sh	$R_2 + \nu_4$	(555)			
803 s	T_1				
853 vs	T_2				
933 vs	T_3				
967 sh	$T_1 + \nu_1$	(976)			
1035 sh	$T_2 + \nu_1$	(1026)			
1104 w	$T_2 + \nu_2$	(1104)			
1178 vw	$T_2 + \nu_3$	(1181)			
1257 m	$T_3 + \nu_3$	(1261)			
1346 vw	$T_1 + \nu_5$	(1352)			
1413 sh	$T_3 + \nu_4$	(1418)			

[a]Data in cm^{-1}. [b]Values in parentheses represent the calculated frequencies based on the vibrational modes listed. [c]From the emission and far-infrared spectra (Table 1).

Table 3. The ^2E_g splitting for *cis*-[Cr^{III}(cyclam)X$_2$]$^{n+}$ complexes

X[a]	Splitting[b]	Anion	Ref.
NH$_3$	83	(BF$_4$)$_2$(NO$_3$)	11
en/2	40	(ClO$_4$)$_3$	12
pn/2	50	(ClO$_4$)$_3$	13
F	169	(ClO$_4$)	14
Cl	139	(Cl)	15
Br	172	(Br)	16
N$_3$	249	(N$_3$)	17
ONO	93	(NO$_2$)	11
ONO$_2$	60	(NO$_3$)	18
NCS	70	(NCS)	This work

[a]en=1,2-diaminoethane; pn=1,2-diaminopropane. [b]Data in cm^{-1}.

have similar frequencies and intensity patterns to those of the ^2E_g components.

The higher energy $^4A_{2g} \rightarrow {}^2T_{2g}$ band was found at 20660 cm^{-1} from the second derivative of the solution absorption spectrum, as shown with a dotted line in Figure 5.

Ligand Field Analysis. The ligand field potential matrix was generated for *cis*-[Cr(cyclam)(NCS)$_2$]$^+$ from the coordinated six nitrogen atoms. The angular positions of ligating six atoms and adjacent two carbons were taken from the X-ray crystal structure[10] of *cis*-[Cr(cyclam)(NCS)$_2$](ClO$_4$), which was determined to be monoclinic with the space group $P2_1/c$. The coordinates were then rotated so as to maximize the projections of the six-coordinated atoms on the Cartesian axes centered on the chromium. The resulting Cartesian and spherical coordinates are shown in Table 4.

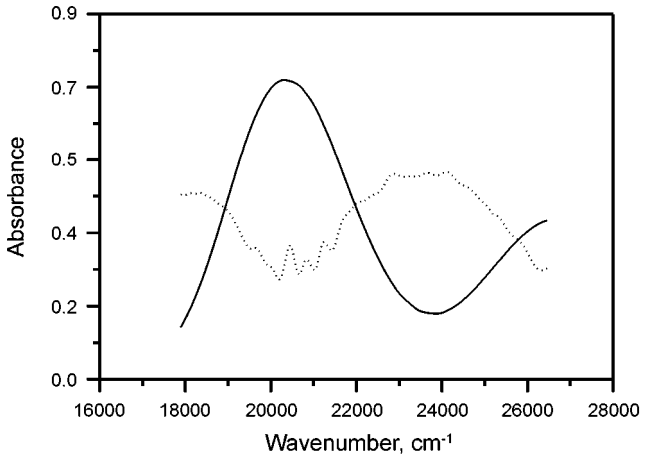

Figure 5. Absorption spectrum (solid line) and second derivative (dotted line) of *cis*-[Cr(cyclam)(NCS)$_2$]$^+$ in aqueous solution at 298 K.

Table 4. Optimized Cartesian and spherical polar coordinates for ligating atoms and adjacent nitrogen atoms in *cis*-[Cr(cyclam)(NCS)$_2$]$^+$[a]

Atom[b]	*x*	*y*	*z*	θ	ϕ	ψ
N_1	2.0624	0.1699	0.1000	90.47	-89.64	0.00
N_2	0.0765	2.0700	-0.0977	179.34	-73.95	0.00
N_3	-2.0628	0.1053	0.1856	87.23	4.71	0.00
N_4	-0.0795	-0.1024	2.0762	92.70	87.88	0.00
N_5	0.0125	-1.9904	-0.0165	84.86	177.08	-87.66
N_6	0.0063	-0.0219	-1.9813	3.57	-127.83	-57.70
C_{11}	0.1486	-3.1443	-0.0207			
C_{12}	-0.0902	-0.1471	-3.1240			

[a]Cartesian coordinates in Å, polar coordinates in degrees. [b]Atomic labeling was adopted from Ref. 10.

Angular overlap model (AOM) parameters provide more chemical insight than crystal field parameters, and are used to interpret the electronic properties.[25] The π-interaction of the isothiocyanate nitrogen with the metal ion was considered to be anisotropic. The anisotropy of metal-ligand π-interaction can be expressed by e_π parameters in two perpendicular directions, denoted $e_{\pi s}$ and $e_{\pi c}$. By rotation of coordinates through the angle ψ, the value of $e_{\pi c}$ can be set to zero, and the π-interaction of the ligand expressed entirely through $e_{\pi s}$. The ligand field analysis was carried out through an optimized fit of experimental to calculated transition energies. Diagonalization of the 120×120 secular matrix yields the doublet and quartet energies with the appropriate degeneracies.[27] The method for determining the eigenvalues and eigenfunctions of a d^3 ion in a ligand field from any number of coordinated atoms has been described.[19] The full set of 120 single-term antisymmetrized product wavefunctions was employed as a basis. The Hamiltonian we have used in the calculation was

$$\hat{H} = \sum_{i<j} \frac{e^2}{r_{ij}} + V_{LF} + \zeta \sum_i l_i \cdot s_i + \alpha_T \sum_i l_i^2 + 2\alpha_T \sum_{i<j} l_i \cdot l_j \quad (1)$$

the terms of which represent the interelectronic repulsion, ligand field potential, and spin-orbit coupling, respectively, with the last two representing the Trees correction.[28] The parameters varied during the optimization were the interelectronic repulsion parameters B, C and the Trees correction parameter α_T, the spin-orbit coupling parameter ζ, plus the AOM parameters e_σ(NCS) and e_π(NCS) for the isothiocyanato nitrogen-chromium, and e_σ(N) for the cyclam nitrogen-chromium. The π-interaction of amine nitrogens with sp^3 hybridization in the cyclam was assumed to be negligible. However, it is noteworthy that the peptide nitrogen with sp^2 hybridization has a weak π-donor character.[29] All parameters, except e_σ(NCS) and e_π(NCS), were constrained to reasonable limits based on the data from other chromium(III) complexes. The seven parameters were used to fit eleven experimental energies: the five $^4A_{2g} \rightarrow \{^2E_g, {}^2T_{1g}\}$ components, identified in Table 5, the lowest energy of the transition to the $^2T_{2g}$ state, the four $^4A_{2g} \rightarrow \{^4T_{2g}, {}^4T_{1g}\}$ components, and the splitting of the ^2E_g state. Eigenvalues were assigned to states within the doublet and quartet manifolds based on an analysis of the corresponding eigenfunctions. The function minimized was

$$f = 10^3 S^2 + 10^2 \Sigma D^2 + 10 T^2 + \Sigma Q^2 \quad (2)$$

where S in the first term is the ^2E_g splitting, and D, T, and Q represent the differences between experimental and calculated $\{^2E_g, {}^2T_{1g}\}$, $^2T_{2g}$, and $\{^4T_{2g}, {}^4T_{1g}\}$ transition energies, respectively. The Powell parallel subspace optimization procedure[30] was used to find the global minimum. The optimization was repeated several times with different sets of starting parameters to verify that the same global minimum was found. The results of the optimization and the parameter set used to generate the best-fit energies are also listed in Table 5. The fit is good for the sharp line transitions. The error margins reported for the best-fit parameters in Table 5 are based only on the propagation of the assumed uncertainties in the observed peak positions.[31] The quartet terms were given a very low weight to reflect the very large uncertainty in their position.

The following values were finally obtained for the ligand

Table 5. Experimental and calculated electronic transition energies for *cis*-[Cr(cyclam)(NCS)$_2$](NCS)[a]

State (O_h)	Exptl	Calcd[b]
^2E_g	13602	13817
	13672	13874
$^2T_{1g}$	14405	14186
	14455	14323
	14535	14437
$^2T_{2g}$	20660	20728
$^4T_{2g}$	19765[c]	19858
	20795[c]	20890
$^4T_{1g}$	25840[c]	25998
	27810[c]	26457

[a]Data in cm^{-1}. [b]e_σ(N) = 7512 ± 45; e_σ(NCS) = 6112 ± 58; e_π(NCS) = 632 ± 28; B = 588 ± 6; C = 2992 ± 38; α_T = 66 ± 10; ζ = 277 ± 54. [c]Obtained from the Gaussian component deconvolution.

field parameters: e_σ(N) = 7512 ± 45, e_σ(NCS) = 6112 ± 58, e_π(NCS) = 632 ± 28, B = 588 ± 6, C = 2992 ± 38, α_1 = 66 ± 10 and ζ = 277 ± 54 cm^{-1}. A ligand field analysis of the sharp-line excitation and broad-band absorption spectra indicates that the isothiocyanato nitrogen has a medium σ- and π-donor properties toward chromium(III) ion. These values for e_σ(NCS) and e_π(NCS) parameters can be compared with the values for other coordinated atoms in the chromium (III) complexes.[32-39] The value of 7512 cm^{-1} for e_σ(N) of the cyclam is slightly larger than 7285 cm^{-1} for the *cis*-[Cr(cyclam)$(N_3)_2$](N_3).[17] It is safe to conclude that the four nitrogen atoms of the macrocyclic ligand cyclam are a strong σ-donor. The AOM parameters can be used in interpreting the photobehavior of transition metal complexes.[40] The observed ^2E_g splitting, 70 cm^{-1} in the excitation spectrum can compared with the values[11-18] of *cis*-diacidochromium (III) complexes with the cyclam, as seen in Table 3. An orbital population analysis yields a configuration of $(xy)^{0.992}(xz)^{1.010}(yz)^{0.972}(x^2\text{-}y^2)^{0.008}(z^2)^{0.018}$ for the lowest component of the ^2E_g state. The relative *d*-orbital ordering from the calculations $E(xy)$ = 154 cm^{-1} < $E(xz)$ = 519 cm^{-1} < $E(yz)$ = 1162 cm^{-1} < $E(x^2\text{-}y^2)$ = 20312 cm^{-1} < $E(z^2)$ = 21389 cm^{-1}. The value of the Racah parameter B is about 64% of the value for a free chromium(III) ion in the gas phase, and it is confirmed that electron repulsions are weaker in the complex than the free ion. The ligand field parameter values reported here appear to be significant, as deduced on the basis of the manifold of sharp-line transitions which were obtained from the well resolved excitation spectrum.

Acknowledgement. This work was supported by Korea Research Foundation Grant (KRF-2002-C00012).

References

1. Ferguson, C. J.; Tobe, M. L. *Inorg. Chem.* **1970**, *9*, 1781.
2. Poon, C. K.; Pun, K. C. *Inorg. Chem.* **1980**, *19*, 568.
3. Sosa, M. E.; Tobe, M. L. *J. Chem. Soc. Dalton Trans.* **1986**, 427.
4. Kutal, C.; Adamson, A. W. *Inorg. Chem.* **1973**, *12*, 1990.
5. Kane-Maguire, N. A. P.; Wallace, K. C.; Miller, D. B. *Inorg. Chem.* **1985**, *24*, 597.
6. Forster, L. S. *Chem. Rev.* **1990**, *90*, 331.
7. Kirk, A. D. *Chem. Rev.* **1999**, *99*, 1607.
8. House, D. A.; Mckee, V. *Inorg. Chem.* **1984**, *23*, 4237.
9. Forsellini, E.; Parasassi, T.; Bombieri, G.; Tobe, M. L.; Sosa, M. E. *Acta Cryst.* **1986**, *C42*, 563.
10. Friesen, D. A.; Quail, J. W.; Waltz, W. L.; Nasheim, R. E. *Acta Cryst.* **1997**, *C53*, 687.
11. Choi, J. H. *Chem. Phys.* **2000**, *256*, 29.
12. Choi, J. H.; Oh, I. G. *Bull. Korean Chem. Soc.* **1993**, *14*, 348.
13. Choi, J. H. *Bull. Korean Chem. Soc.* **1993**, *14*, 118.
14. Choi, J. H.; Hong, Y. P.; Park, Y. C.; Ryoo, K. S. *J. Photosci.* **2000**, *7*, 21.
15. Choi, J. H. *J. Korean Chem. Soc.* **1995**, *39*, 501.
16. Choi, J. H. *J. Photosci.* **1997**, *4*, 127.
17. Choi, J. H. *Spectrochim. Acta* **2000**, *56A*, 1653.
18. Choi, J. H. *Bull. Korean Chem. Soc.* **1997**, *18*, 819.
19. Hoggard, P. E. *Coord. Chem. Rev.* **1986**, *70*, 85.
20. Choi, J. H. *Bull. Korean Chem. Soc.* **1994**, *15*, 145.
21. Nakamoto, K. *Infrared and Raman Spectra of Inorganic and Coordination Compounds, Part B*, 5th Ed.; John Wiley & Sons: New York, 1997.
22. Choi, J. H. *Bull. Korean Chem. Soc.* **1998**, *19*, 575.
23. Choi, J. H. *Bull. Korean Chem. Soc.* **1999**, *20*, 81.
24. Choi, J. H.; Hong, Y. P.; Park, Y. C.; Lee, S. H.; Ryoo, K. S. *Bull. Korean Chem. Soc.* **2001**, *22*, 107.
25. Lever, A. B. P. *Inorganic Electronic Spectroscopy*, 2nd Ed.; Elsevier: Amsterdam, 1984.
26. *GRAMS 32 V5.21*; Galactic Industries Corporation, Salem, NH 03079, USA.
27. Smith, B. T.; Boyle, J. M.; Dongarra, J. J.; Garbow, B. S.; Ikebe, Y.; Klema, V. C.; Moler, C. B. *Matrix Eigensystem Routines-EISPACK Guide*; Spring-Verlag: Berlin, 1976.
28. Trees, R. E. *Phys. Rev.* **1951**, *83*, 756.
29. Choi, J. H.; Hoggard, P. E. *Polyhedron* **1992**, *11*, 2399.
30. Kuester, J. L.; Mize, J. H. *Optimization Techniques with Fortran*; McGraw-Hill: New York, 1973.
31. Clifford, A. A. *Multivariate Error Analysis*; Wiley-Hasted: New York, 1973.
32. Hoggard, P. E. *Top. Curr. Chem.* **1994**, *171*, 114.
33. Schönherr, T. *Top. Curr. Chem.* **1997**, *191*, 87.
34. Choi, J. H.; Park, Y. C.; Kim, H. S. *J. Photosci.* **2000**, *7*, 97.
35. Choi, J. H.; Hong, Y. P.; Park, Y. C. *J. Korean Chem. Soc.* **2001**, *45*, 436.
36. Choi, J. H. *Bull. Korean Chem. Soc.* **1999**, *20*, 436.
37. Choi, J. H. *J. Photosci.* **1996**, *3*, 43.
38. Choi, J. H.; Hong, Y. P.; Park, Y. C. *Spectrochim. Acta* **2002**, *58A*, 1599.
39. Choi, J. H. *J. Photosci.* **2002**, *9*, 51.
40. Vanquickenborne, L. G.; Ceulemans, A. *Coord. Chem. Rev.* **1983**, *48*, 157.